ORIGINAL ARTICLE

Involvement of the Claustrum in Human Epileptic Seizures

Rene Andrade Machado, MD[1]; Jennifer Meylor, MD[2]

[1]Nemours's Children Hospital, Department of Pediatric, Division of Neurology, Orlando, Florida, United States.
[2]Medical College of Wisconsin, Department of Neurology, Division of Pediatric Neurology, Milwaukee, WI, United States

Received: 3 Mar 2025
Accepted: 17 Feb 2026
Published: 1 Sep 2026

Keywords:

Epilepsy
Stereoelectroencephalography
Intracranial electrodes
Epileptogenesis
Epilepsy surgery
High frequency oscillations

ABSTRACT

Objectives: We aimed to assess if the claustrum is involved in seizure networks in humans with epilepsy.
Materials and Methods: We identified eight patients submitted for presurgical evaluation with stereoelectroencephalography (SEEG) recordings from the claustrum from 2016-2022. Demographic, paraclinical, and outcome data (Engel Classification) was collected from retrospective chart review. We analyzed the ictal and interictal pattern as well as high frequency oscillations (HFOs) in the claustrum.
Results: The ictal onset zone was in the temporal lobe in 87% (n=7) of patients and the cingulate cortex in 12% (n=1). A total of 25 seizures were detected and 96% (n=24) involved the claustrum cortex. Of those seizures involving the claustrum, 88% (n=21) were involved before the rest of the electrodes. Two ictal onset patterns were identified: slow potential shift with HFOs were found in 46% (n=11) of seizures and rhythmic spikes <13 hz were found in 54% of seizures (n=13). The ictal pattern in the claustrum was synchronous with the ictal onset zone in 41% (n=10) seizures, however, in four patients with status epilepticus, the claustrum was noted to stop discharging just before ictal onset. The interictal pattern included high-amplitude slow waves with or without HFOs. HFOs were identified in the claustrum in 83% (n=20) of post-ictal periods. All patients had poor outcomes following surgical resection (Engel Class III-IV).
Conclusions: Our study suggests that the claustrum is often involved during seizures arising from the temporal lobe and cingulate cortexes and could play a role in modulation of the epileptogenic network.

How to cite this article: Andrade Machado R, Meylor J. Involvement of the Claustrum in Human Epileptic Seizures. Iran J Child Neurol. 2026;20(4):e3. https://doi.org/10.22037/ijcn.V20I4.47731

Introduction

The *claustrum* is a thin, irregular sheet of grey matter concealed between the inner surface of the neocortex.(1, 2) Over the past decades there have been multiple roles proposed for the claustrum including movement organization, visual motor coordination, and memory processing.(3, 4) More recent studies have shown that the claustrum has extensive connectivity within the limbic system and entire cerebral cortex, implicating the claustrum in more higher order processing.(5, 6) The specific role of the claustrum in seizure generation and propagation remains unknown.

Literature in animal models has proposed a role for the claustrum in modulation of epileptic networks. (7-9) Rodent models of epilepsy have aimed to define different claustrum subregions implicated in seizure generation and propagation.(10) Literature in human subjects has only recently begun to uncover the role of the claustrum. Structural magnetic resonance imaging (MRI) studies have identified hyperintensities and edema of the claustrum during the postictal period in patients with seizures and status epilepticus, providing evidence of its involvement in seizures through the regulation of cortical excitability.(11-13) However, studies of neuropathological review have found no

Corresponding Author:
Rene Andrade Machado
Email: rene.andrademachado@nemours.org

This work is licensed under a Creative Commons Attribution-NonCommercial 4.0 International (CC BY-NC 4.0) which allows users to read, copy, distribute and make derivative works for non-commercial purposes from the material, as long as the author of the original work is cited properly.

structural abnormalities in the claustrum of patients with chronic epilepsy and status epilepticus, so it remains possible that these radiographic changes in the claustrum could indicate a broader network dysfunction rather than a focal structural abnormality.(11, 12)

Despite considerable research on the claustrum in animal models and human patients with status epilepticus, the specific role of the claustrum in patients with refractory epilepsy remains largely unexplored, highlighting a critical gap in the literature that our study aims to address. A study by Mohamad et al., 2014 documented the role of the claustrum in consciousness, but the role of the claustrum in the interictal activity of patients with epilepsy remained to be elaborated.(14)

Our primary objective is to use the high spatial and temporal resolution of intracranial stereoelectroencephalography (SEEG) recordings in patients with refractory epilepsy to investigate the role of the claustrum in seizure propagation and maintenance. This study looked at the ictal and interictal features of the claustrum, as well as the timing of claustrum involvement compared to seizure onset. We hypothesized that the claustrum has heightened connectivity with the ictal onset zone and modulates seizure activity.

The significance of this study is to expand our knowledge of the role of subcortical structures in the modulation of ictal activity during seizures. Thus, this study presents the possibility of initiating new prospective studies targeting the claustrum and determining the role of the ictal pattern in patients with refractory epilepsy.

Materials & Methods

Subjects

A descriptive, observational study was performed with retrospective data collected from patients at Children's Hospital of Wisconsin between 2016 and 2022. We reviewed 55 pediatric patients who underwent surgical resections after SEEG evaluations for the treatment of medically refractory epilepsy. Due to the claustrum abutting the external capsule, this structure is not typically a target in our institution during routine SEEG electrode implantation. Thus, the claustrum was unintentionally targeted in this study. Inclusion criteria were as follows: (1) at least one electrode with one contact in the claustrum, (2) a band of white matter seen radiographically between the contact located in the claustrum and the nearby insular cortex, and (3) age between 3-17 given the age restrictions of SEEG implantation. Exclusion criteria included patients with evidence of insular lesions on MRI, insular hypometabolism on positron emission tomography (PET) scan or insular-onset seizures, (4) patients with structural lesions in parietal, occipital, and frontal lobes, or (5) patients with auras suggestive of extratemporal epilepsy.

Data Collection

Demographic data including age and etiology of epilepsy were recorded from the clinical chart. All patients underwent a presurgical evaluation including neurological examination, video-electroencephalogram evaluation, neurocognitive testing, intracranial PET results, and brain MRI results. In this study, all patients required invasive SEEG recordings after the standard noninvasive presurgical evaluation phase. SEEG was indicated for any of the following reasons: when presurgical evaluation data were non-concordant regarding localized and lateralized epileptogenic zone (EZ) and the EZ was suspected to be larger than the lesion, when extra-temporal structures were suspected to be involved in temporal lobe seizures, when bilateral onset was suspected, or when an eloquent area was suspected to be involved.(15) The ictal semiology was analyzed by reviewing the videos of seizures captured during intracranial evaluation. The post-surgical outcome was assessed according to Engels's seizure outcome.(16) At least three typical seizures in every patient were evaluated.

Stereotactic Electroencephalography Recordings

The decision regarding the anatomic positioning of electrodes was established in each patient based on available noninvasive data and hypotheses regarding the localization of the EZ. Electrode positions were, therefore, chosen according to the individual clinical characteristics of each case. SEEG recordings were performed according to the standard protocol. Between eight and twenty multiple-contact Ad-Tech electrodes (length 2 mm, diameter 1.1 mm, spacing 5 mm with platinum contacts, numbered and color-coded for identification, 19 cm depth indicator marker, inner wire stylet) were implanted intracranially in the mesial temporal lobe structures and the temporal neocortex, as well as the extra-temporal areas when required. These electrodes were implanted using the standard stereotactic technique with the assistance of a stereotactic robot drilling 2.5 mm diameter holes. Depending on patient characteristics in our center, both orthogonal and oblique orientations permit dynamic recording of cortical, subcortical, lateral, intermediate, and deep structures. All these elements allow an adequate 3-dimensional view of the ictal onset zone and the surrounding structures of interest, and upon recording, the spatiotemporal interaction of these regions when seizures occur. For the purpose of this

study, we present patients with both an orthogonal and oblique approach in the insular cortex.

Electrodes were numbered between 5 and 15, and depending on individual case characteristics were placed orthogonally or obliquely during general anesthesia. Postimplantation electrode localization was performed after fusing the postoperative thin-sliced computed tomography (CT) scan with the preoperative structural MRI through dedicated software. Electrodes are identified by a letter of the alphabet (there is no standard labeling for each location in our institution). When electrodes are located on the left hemisphere, an asterisk following the letter is used, for instance (A*) (Figure 1)

The SEEG signal was high-pass filtered at 0.016 Hz and low-pass filtered at 1000 Hz and recorded on a 128-channel Micromed system (DaVinci, Italy) at a sampling rate of 2000 Hz. A high-pass filter was set off to assess slow potential shift (SPS). Within 24 hours following the operation, a routine brain MRI (1.0-mm slices) was carried out to confirm each electrode's location and assess if bleeding was present. Final electrode locations and their relationship with lesional tissue were determined on the postimplantation brain CT scan/MRI see below (determination of Claustrum Involvement). Alternatively, these data were obtained by combining the information from the reconstructed position of the electrodes from the Neuronavigation system, a postimplantation head CT, and a post-explantation brain MRI.

Postoperatively, a long-term video-SEEG was recorded to capture each patient's habitual seizures; during this time, antiseizure medications were either partially or entirely withdrawn. The SEEG was analyzed through visual inspection. An experienced neurophysiologist (author RAM) reviewed the SEEG data.

Determination of Claustrum Involvement:

Locating Intracranial Electrode Contacts

To analyze the recording typically found out the position of each contact relative to brain structures. Since the brain is best visualized by a pre-implantation magnetic resonance (MR) image whereas the electrode contact locations are best visualized in a post-implantation computed tomography (CT) images. A post implantation CT scan were obtained to use the skull, and to aligned to MR-space. This accomplishes our goal of obtaining contact locations in MR-space (which is where the brain structures are best determined using the FreeSurfer MRI reconstruction). Thus, T1 weighted imaging were aligned to anterior commissure and posterior commissure (ACPC). Brain Imaging Data Structure (BIDS) standard requires that coordinates be aligned to the anterior commissure and posterior commissure (ACPC-aligned) with this we made the “mri” coordinate frame an ACPC coordinate frame. This was done using Freesurfer’s Freeview and then interact with the graphical user interface. Later, a freesurfer reconstruction was performed. This process segmented out the brain from the rest of the MR image and determined which voxels correspond to each brain area based on a template deformation. After that, we estimated the “head” coordinate transform. Using MNE stores digitization montages in a coordinate frame called “head” (defined by fiducial points), we got an estimate of the location of the fiducial points for the subject using the Talairach transform. Now, that the CT and the MR are in the same space we determined the location of each electrode contact in the individual subject’s anatomical space (T1-space). To do this, we used the MNE intracranial electrode location graphical user interface. After that, electrode contacts were considered to be in the claustrum if located within the visible borders of the claustrum on neuroimaging and were consistent with the localization coordinate in the MNI atlas. For this report, the dorsal and ventral claustrum were divided by an imaginary line that crosses the central insular sulcus (Figure 2). Figures 2.1 and 2.2 show different electrodes with at least one contact in the claustrum different approaches were used (orthogonal and oblique). To better determine that the recorded activity was representative of claustrum activity we demonstrated that the activity of the contact within the claustrum is different from the surrounding contacts. To record this unique signal, we used a monopolar montage with a reference montage. The reference contact was an electrode that did not show artifact or interictal activity and was not part of the ictal pattern. Reference contacts were located within the white matter.

Measurements

For electrodes placed using the neuromate robot, localization errors were calculated by fusing the planned trajectories to the postoperative CT images. Stereotactic coordinates were taken from the electrode tip and from the planned target. For the cortical entry point, the stereotactic coordinates of the electrode and the planned trajectory were taken using images coaxial to the planned trajectories at the image slice where the electrode penetrated the cortical surface. The localization error was calculated using the Euclidean distance between stereotactic points.

Ictal Recordings

The ictal onset was considered the first change in the intracranial SEEG which had an apparent change

from background, and it was sustained and followed by a spread pattern. The involved anatomic structure was determined by correlating the electrode contact that showed the first unequivocal ictal onset change with the radiographic structure where it was implanted. Then, the spread zone was determined as the contact involved in a sustained ictal activity at least 500 milliseconds after seizure ictal onset. The sensitivity for the channel recording of electrodes within the claustrum was changed to a sensitivity between 150 microvolts (uV) to 60 uV. We determined further if the ictal change in the claustrum occurred in the ventral or dorsal claustrum, as well as determined the ictal frequency, pattern morphology, and built-up pattern observed in the claustrum. We also evaluated the temporal relationship of the ictal pattern in the claustrum in relation to the ictal onset in other temporal lobe structures. Awake and sleep epochs were analyzed. A segment of SEEG one hour before and one hour after a seizure was analyzed to evaluate the interictal activity in the claustrum. The filters were set as follows: Low-Frequency Filter (LFF) 0.016 Hz, High-Frequency Filter (HFF) 1000 Hz, Notch ON, sampling 2000 Hz. Sensitivity was between 40-30 uV.

To ensure that seizure-onset assessment was carried out blindly to patient clinical data, one neurophysiologist (RAM) reviewed the intracranial EEGs independently, determined the time and site of seizure onset, and described the frequency, amplitude, and morphology of the intracranial EEG discharge. The ictal onset zone (SOZ) was the first unequivocal intracranial EEG sign of change from the background that led to a clear seizure discharge without returning to background activity (first unequivocal ictal intracranial EEG change). The name and contact numbers of the electrode or electrodes involved were noted. The ictal onset and early spread of intracranial EEG were classified based on the frequency, amplitude, morphology, and presence of slow potential shifts (SPS). Standardized terminology was used from the 2021 American Clinical Neurophysiology Society's Standardized Critical Care EEG report.(17) For the purpose of this study more than three seizures in one hour was considered a cluster of seizures if patients did not have this frequency of electroclinical seizure reported before.

High-Frequency Oscillations

High-frequency oscillations (HFOs) were analyzed by visual inspection in the seizure onset zone and the claustrum and Morlet wavelet transform. The filters were set as follows: LFF 80 Hz, HFF 1000 Hz, Notch ON, sampling 2000 Hz. Sensitivity was between 40-30 uV.

Quantitative analysis of the EEG

We used Fast Fourier transformation (FFT) for spectral analysis of quantitative EEG ranges without artifacts. Spectral analysis facilitates the determination of the distribution of power according to frequency, which provides information about the frequency content of a signal. The absolute (μV2) and relative (%) power, mean frequency, inter- and intrahemispheric coherence, and total spectral power were calculated for the delta (0.5-4 Hz), theta (4-8 Hz), alpha (8-13 Hz), beta (13-30 Hz), high beta (25-30 Hz), gamma-1 (31-80 Hz), ripples (80-250), and HFOs >250 Hz frequency bands. FFT was used to calculate the background frequency. A Density Spectral Assay (DSA) graph was computed from five minutes of raw data using inbuilt settings in the software and was correlated with the visual presence of seizures and changes in background frequencies. We used Time-Frequency [TF] Analysis of the SEEG signal to evaluate the ictal pattern and the presence of HFOs. The electrical activity recorded by the selected contacts was analyzed from the onset of fast activity. We performed a TF analysis on the extracted segments from channels of interest using the Morlet wavelet transform (MWT). For this quantitative visual analysis, we used the MWT provided by Brainstorm with a time resolution of five seconds for a central frequency of 1Hz, which generated TF maps with 50 frequency bins in a logarithmic scale from 1 to 200Hz. We identified the onset of the fast activity via visual analysis of the TF maps and measured the frequency of the fast activity. As the terminology for ictal fast activity varies among studies in the literature, we used the term HFOs for brain activity that exceeds 80 Hz.

Statistical analysis

Data are presented as numbers and percentages in tables and figures. All analyses were performed with Statistic Version 6.0.

IRB Approval

This retrospective study was approved by our Institutional Review Board [PRO00049035**].**

Results

Demographics, Phase II Surgical Evaluation, and Outcomes

Eight total patients were identified with at least one electrode in the claustrum (Table 1). Median age was 12.9 years with a predominance of male gender (87.5%, n=7). The ictal onset zone was in the temporal lobe for 87.5% of patients (n=7), except for one patient who had an ictal onset zone in the subgenual cingulate cortex. Two patients had temporal plus epilepsy,

including an ictal onset zone also in the insular cortex or the frontal region. Seizure semiology can be found in Table 1. The etiology of epilepsy for our cohort included gliosis (37.5 %, n=3), glioma (25 %, n=2), hippocampal sclerosis (12.5%, n=1), FCD type IIa (12.5%, n=1), and unknown (12.5%, n=1). Surgical resection following SEEG evaluation included temporal lobectomy (62.5%, n=5), frontotemporal resection (12.5%, n=1), temporo-insular cortex resection (12.5%, n=1) and one patient was treated with interstitial laser ablation of the cingulate gyrus. Seventy-five percent of electrographic recordings were obtained from the left claustrum. The electrode recording was located in seven out of eight patients in the ventral claustrum (table 1). Interestingly, 100 % of patients had a poor postsurgical seizure outcome (Engel's scale III or IV) (table 1).

Table 1: Demographics, presurgical planning data, SEEG, surgery types, and surgical outcomes of studied patients

Demographics, presurgical planning data, SEEG, surgery types, and surgical outcomes	
	N (%) (total = 8)
Male	7 (87.5)
Age (In Years)	
9-17	8 (100)
Etiology of Epilepsy	
Glioma	2 (25)
Gliosis	3 (37.5)
Hippocampal Sclerosis	1 (12.5)
FCD Type IIa	1 (12.5)
Unknown	1 (12.5)
Seizure Semiology	
Impaired Awareness to CTC	5 (62.5)
Auditory Hallucinations to	1 (12.5)
Hypermotor Automatisms	2 (25)
Recording Location	
Left Claustrum	Left Claustrum
Ventral Claustrum	Ventral
Seizure Onset Zone	
Hippocampus	3 (37.5)
Cingulate Cortex	1 (12.5)
Orbitofrontal	2 (25)
Amygdala	1 (12.5)
MTG	1 (12.5)
Resection	
Left Temporal Lobectomy	3 (37.5)
Right Temporal Lobectomy	2 (25)
Cingulate gyrus [subgennual	1 (12.5)
Frontotemporal	1 (12.5)
Temporo-insular cortex	1 (12.5)
Engel Classification (I-IV)	
III	6 (75)
IV	2 (25)

Claustrum Recordings

Interictal findings

The background activity recorded within the claustrum consisted of low amplitude 50-100 uV ranging from theta to alpha-beta activity, typically from 5.1 to 29 Hz in 7 out of 8 patients (87.5%) (Supplementary material 1). Rarely delta activity was noted (12.5 %, n=1) [Table 2]. Supplementary material 2 shows FFT in 2 seconds of recording in a patient with orthogonal implantation. Electrode PI1 is in the claustrum, and PI2 and PI3 are located in the insular cortex, which shows a different range of frequencies. PI1 (see figure 2.1), located in the claustrum, shows a peak at the theta frequency (6 Hz) while the insular cortex shows alpha frequency activity (supplementary file 2). Supplementary file 3 shows three different electrodes, NL1, JL1, and JL2. NL1 is an electrode situated in the anterior cingulate cortex. JL1 is in the anterior and ventral claustrum, and JL2 is within the insula (see Figure 2.3). The time-frequency analysis shows a continuous delta activity in JL1 as compared to JL2 (insular cortex).

Table 2. Claustrum SEEG Recordings

Claustrum SEEG Recordings	N (%) (total = 8)
Recording Location	
Left Claustrum	6 (75)
Ventral Claustrum	7 (86.5)
Background Recording	
Low amplitude alpha-beta activity	4 (50)
Low amplitude theta activity	3 (37.5)
Delta activity (<3 Hz) [75-150 uV]	1 (12.5)
Interictal Recording	
Delta activity + HFOs	2 (25)
Sharp Waves	4 (50)
High amplitude spikes ± HFOs	5 (62.5)
Synchronous interictal activity between claustrum and SOZ	5 (62.5%)
Synchronous spike/HFOs activity with slow wave of spike and slow complexes of the SOZ	5 (62.5%)
Ictal Recordings	N (%) (total=25)
Rhythmic activity (<13 Hz)	11 (41.7)
SPS and HFOs	13 (54.2)
Synchronous onset with SOZ***	10 (41.7)
Buildup of low amplitude fast activity	16 (66.7)
Buildup of rhythmic spikes < 13 Hz	8 (33.3)
Temporal onset before other electrodes not involved in the ictal onset	21 (87.5)
Continuous activity through status epilepticus or recurrent seizures	0 (0)
Postictal Recordings	
Postictal suppression	11 (45.8)
Synchronous termination with SOZ	11 (45.8)
Periodic HFOs	15 (62.5)

Hz=Hertz, uV=micro-volt, HFO= High Frequency Oscillation, SPS= slow potential shift, SOZ=Seizure Onset Zone

Interictal activity was characterized by high amplitude slow waves with or without superimposed HFOs (supplementary file 3) (62.5 %, n=5). Interictal sharps were found in 50% of patients (n=4). The interictal activity in the claustrum appeared synchronously with the interictal activity in the ictal onset zone in 62.5% of patients (n=5) (supplementary file 4). The spike or HFOs in the claustrum was noted to be synchronous with the slow wave of spike and wave complexes in the ictal onset zone (62.5 %, n=5) (supplementary file 5). Supplementary file 6 shows periodic epileptiform activity in the hippocampus and synchronous periodic HFOs around 200 Hz in the claustrum. Periodic discharges were seen in the insular cortex but it never correspond with HFOs (reference the rectangle in contact PI1 (see figure 1 for localization) (table 2).

ictal findings

A total of twenty-five seizures were analyzed (table 2). The seizures involved the claustrum in 96% of the time (n=24). Two ictal onset patterns were identified: (1) SPS and HFOs found (54.1%, n=13) and (2) rhythmic spikes <13 Hz (45.figure 3 A8%, n=11) (Figure 3a). Figure 3 B shows the synchronous termination of seizures among the claustrum and the rest of the electrodes. However, see postictal discharges in the claustrum. The ictal pattern in the claustrum appeared synchronously with the ictal onset zone in just less than half (41.7%, n=10) of recorded seizures (Figure 3 c). The buildup pattern comprised low-amplitude fast activity (66.7%, n=16) of seizures (Figures 3A and 3B). In 21 out of 24 seizures (87.5%), the claustrum was involved before the rest of the electrodes (Figure 3 D). Note that the claustrum stopped discharging, and the ictal onset zone continues with periodic discharges (Figure 3 D). The ictal pattern ended synchronously in the SOZ and the claustrum in 45.8% of seizures (n=11). Periodic HFOs were detected during the postictal period in the claustrum for 62.5% of seizures (n=15) (Figure 3 E). Interestingly, in four patients we detected clusters of seizures. In these cases, the claustrum stopped discharging before the SOZ (Figure 3 F).

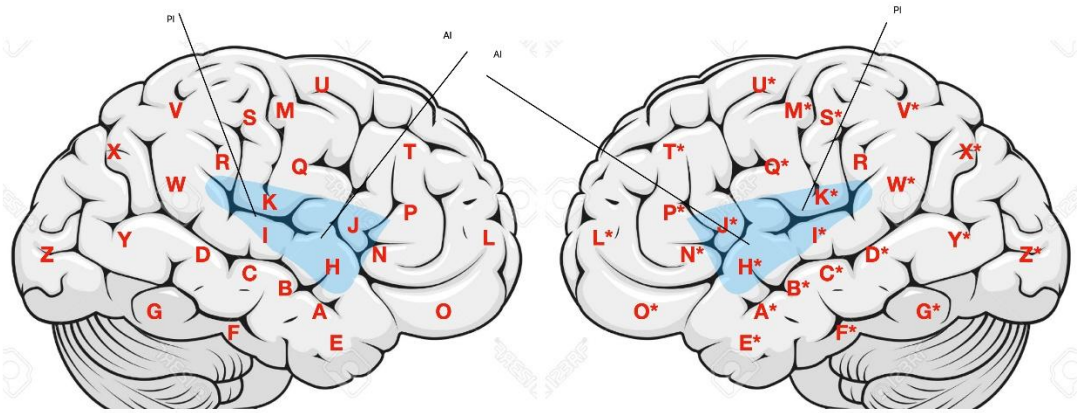


Figure 1: Localization of SEEG electrodes in our center (schematic and nomenclature)

Discussion

This is the first study to detail SEEG findings of the claustrum in patients with refractory epilepsy. Previous literature reporting the characteristics involvement of the claustrum during seizures was mostly performed in animal models, with minimal case reports of radiographic or histologic findings in the human claustrum after seizures(18-20). This study provides unique data to the scientific community, including direct intracranial recordings from the claustrum.

The temporal lobe is known to have extensive connections with the claustrum cortex(1). A key finding of this study was that in almost all the seizures recorded (96%), the claustrum was involved. These results mirror those performed in animal models showing the early involvement of claustrum in seizures coming from the limbic system(2, 9, 21, 22). We found that both the dorsal and ventral claustrum could be involved in seizure evolution. The ictal signature of the claustrum ranged from the buildup of low-amplitude fast activity to the buildup of rhythmic spikes (<13 Hz).

Our study also provides information on the temporal relationship between claustrum activation and the rest of the epileptogenic network. Claustrum spikes or HFOs were noted to be synchronous with the slow wave of spike and wave complexes in the epileptogenic zone in 62.5% of patients. The ictal pattern in the claustrum appeared synchronous with seizure onset zone (SOZ) in 62.5% of patients. This synchrony does not appear to be related to the

localization of the ictal onset zone since the activity was noted in patients with seizures of both the temporal lobe and cingulate gyrus. This correlates with previous animal model research that described ictal activity preceding and simultaneous in the claustrum and hippocampus during seizures in rat models.(8) Sheerin et al. 2004 found a possible synergistic relationship between the claustrum and the amygdala. They described the role of claustrum lesions in rats with amygdala kindling and noted that seizure duration shortened when the claustrum was destroyed in this model. Furthermore, there was evidence of transfer of kindling from the amygdala to the claustrum, again supporting the idea of an extensive network of connections involving the claustrum that lead to seizure propagation.(9) Wada et al., 1997 noted that with similar amygdala kindling models if there was a unilateral claustrum lesion, the seizures would still propagate to the contralateral hemisphere.(7) Our findings could support this theory of early involvement of the claustrum and the role in the initiation and propagation of seizures in this model.

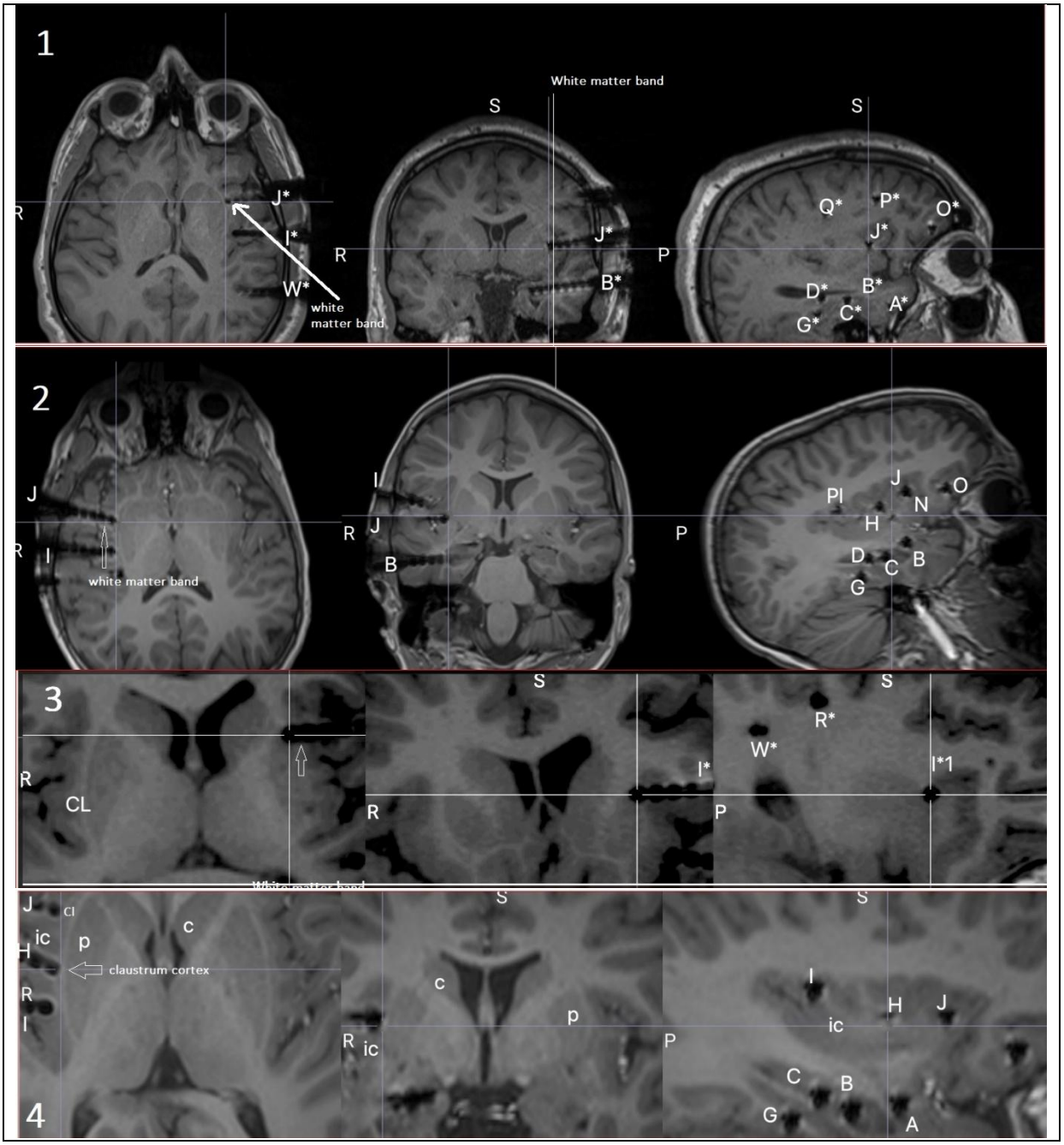


Figure 2.1. The coronal and axial T1 weighted brain MRI of two patients (Figure 2.1 A and B). Coronal MRI showed an SEEG oblique electrode (PI) with the first contact in the ventral clastrum (PI) (A). Axial view showing contact 1 of PI electrode in the claustrum (claustrum was circle with red color) (figure 2.1B). Figure 2.1 C Brain slice showing anatomic relationship between insular cortex, Claustrum and Putamen nucleus]. Electrode J* with the first contact in Claustrum and second in insular cortex [figure 2.1 D].Figure 2.2.

Axial T1 weighted brain MRI showed white matter between the electrode and the insular cortex (white arrow). Axial brain MRI showed that the left claustrum was marked with grey cross lines. Contact one electrode J* in the claustrum. Figure 2.3. Axial, Coronal and sagittal T1 weighted MRI imaging (arrow shows insular cortex)[vertical and horizonal line crosses in the claustrum].
Figure 2.4 a and b Coronal T1 weight MRI showing a different patient with orthogonal implantation of one electrode (called H and I) with the first contact in the ventral claustrum [anterior H and posterior I] and second contact in the insular cortex. ic =insular cortex, Cl =claustrum, C = caudate nucleus, P and Pu = Putaminal Nucleus.

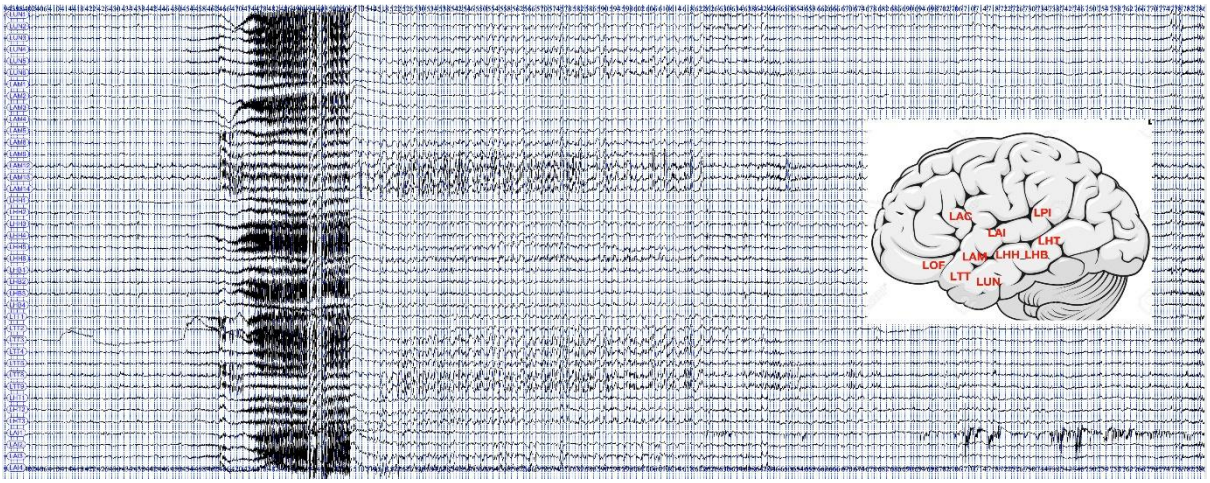


Figure 3A. Vertical lines in the EEG represent seconds of recording. Left temporal lobe seizure. Note the evolution from the interictal to ictal pattern. The ictal onset consists of 4-5 hz rhythmic spike in electrode TT1-2 (uncus) see vertical line at (460 seconds) following by rhythmic spike in electrodes LAM5-14 (middle temporal gyrus) and in LTT5-9 (temporal pole) simultaneously, low amplitude sharp wave discharges are seen in electrode AI contact 1. This is followed by a diffuse low voltage fast activity involving electrodes in the left uncus, temporal pole, amygdala, hippocampus and middle temporal gyrus, claustrum and insular cortex. Ictal evolution is characterized by diffuse 3-5 Hz rhythmic spike and wave discharges lasting 50 seconds and finishing with diffuse slowing. Note the synchronous termination of AI1 and the rest of electrodes.

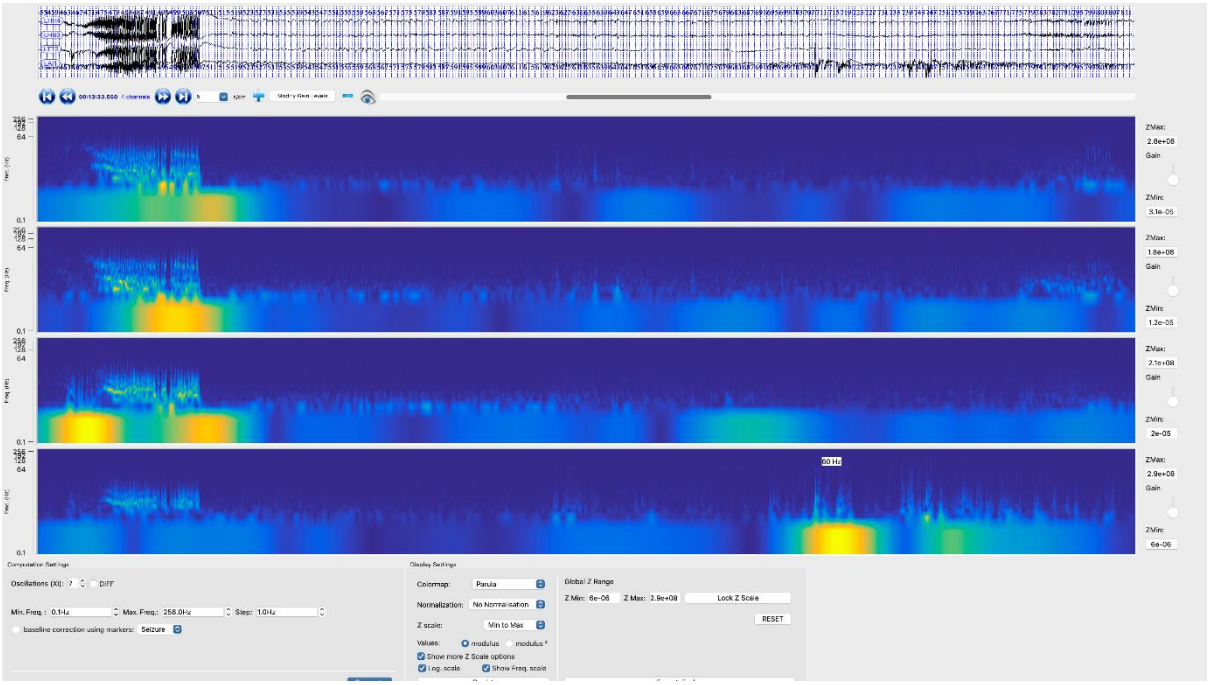


Figure 3 B: Time-frequency analysis. Claustrum postictal discharges
The time frequency analysis shows 5 minutes of seeg recording. Vertical lines in the EEG represent seconds of recording. Only electrodes AI contact 1, LTT2, LHB3 and LHH4 were chosen for the analysis. Observe in yellow and blue the presence of infraslow activity. During the postictal period the claustrum continues showing epileptiform discharges and fast frequency oscillations while no epileptiform activity is seen in the rest of the electrodes.

Interestingly, an alternate temporal model of claustrum activity was also revealed during episodes of clustering of seizures in our cohort. It was noted that if seizure activity was recurrent, the activity in the

claustrum stopped discharging just before the activity was detected in the SOZ (Figure 3D). In the Figure 3D (the circle) shows an example of ictal suppression following claustrum discharges on SEEG. We postulate that some inhibitory activity of the claustrum in seizure evolution is needed to stop ongoing seizure activity. Previous data from animal model studies, have suggested an inhibitory role of the claustrum. Electrical stimulation of the claustrum in cats was noted to cause brief, fast bursts of neuronal activity followed directly by a prolonged suppression in the oculomotor frontal eye field and primary visual cortex.(3, 23) These effects could be attributed to a feedforward inhibitory loop originating in the claustrum.(24)

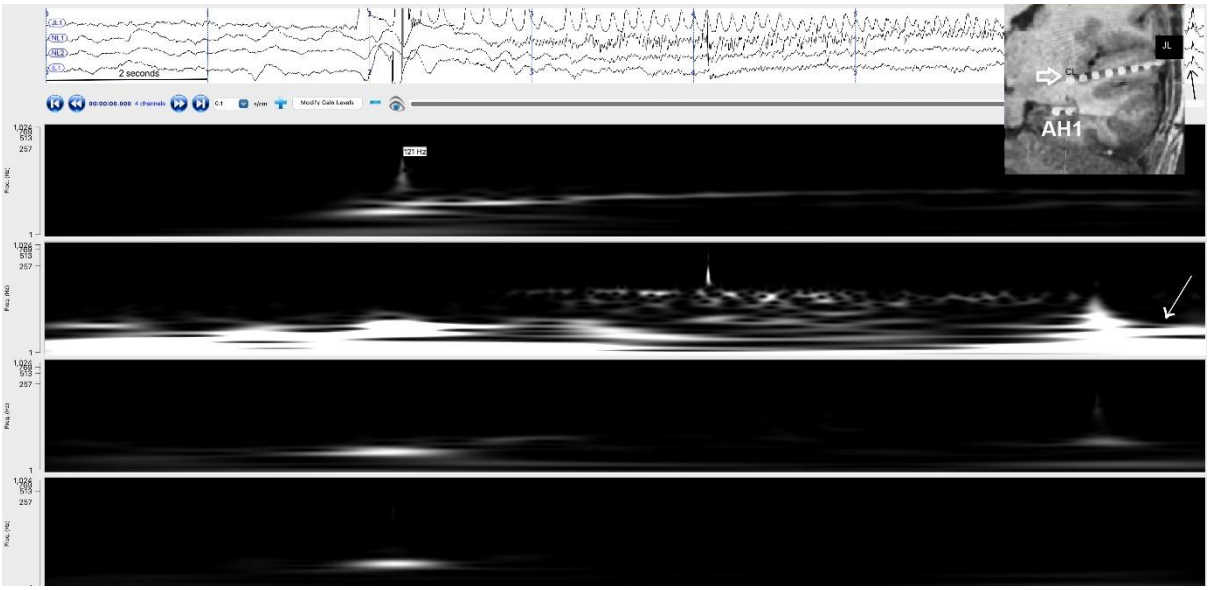


Figure 3C. Synchronous onset between claustrum and cingulate cortex.
This is a 12-year-old patient with brief hypermotor seizures (10 seconds). See sudden onset of HFO in the claustrum synchronously with infra low activity in the cingulate cortex. This pattern evolved to low voltage fast activity in the cingulate cortex and then rhythmic 13 hz activity that terminated after 11 seconds. Note the synchronous ictal onset between claustrum (JL1) and NL1 in the anterior cingulate cortex (white arrows). The sustained ictal activity in the claustrum is associated with early termination of the ictal pattern in the cingulate cortex (black arrows shown in the SEEG recording and white arrows in the time-frequency analysis).

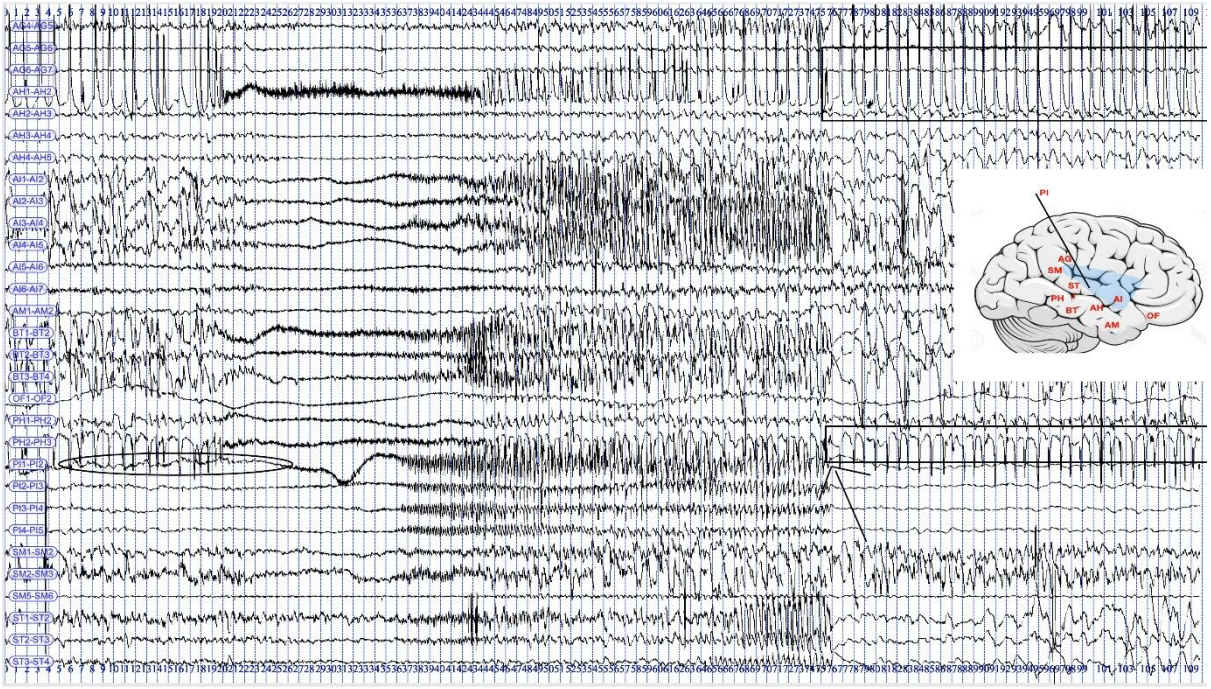


Figure 3D. Claustrum involvement [PI1 electrode] precedes the involvement of other electrodes during seizure evolution. The patient is a 13-year-old with a focal seizure with impaired awareness. AG means angular gyrus, AH hippocampal head, AI anterior insular cortex, OF orbitofrontal cortex, PI indicates the posterior insular cortex (contact one is in the claustrum), SM supramarginal gyrus. PH is parahipocampus and inferior temporal gyrus. The ictal pattern is characterized by the sudden onset of high amplitude 1-2 Hz periodic spike in the hippocampus

head (AH1-2) and Parahipocampus PH1-2. At the same time, periodic HFO appeared in the claustrum that precedes the diffuse low voltage fast activity seen in electrodes PI2-5, SM2-SM6, ST2-to ST6, BT1-BT4, OF1-2, AI1-5, AG 4-6 lasting 12-13 seconds. The ictal pattern evolved into diffuse 10-13 Hz rhythmic spike discharges lasting 76 seconds, followed by attenuation in PI1-5 (parietal cortex, insular cortex, claustrum, angular gyrus, and middle temporal gyrus). Note (black arrow) that the claustrum discharges end abruptly, but the hippocampus and parahippocampus continue showing periodic high amplitude spikes and wave discharges. In the basal temporal structures BT and superior temporal gyrus AI 3-6 and insular cortex AI1, high amplitude delta activity with superimposed faster frequencies is noted during the postictal period.

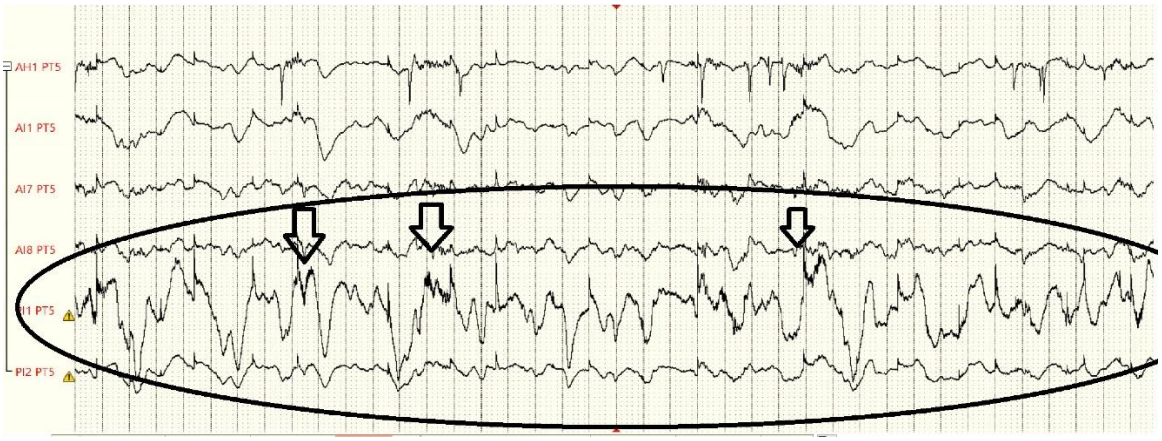


Figure 3E. High-frequency oscillation of the claustrum during the postictal period.
The patient is a 13-year-old with a focal seizure with impaired awareness (postictal period). AH represent hippocampal head, AI anterior insular cortex, PI indicates the posterior insular cortex (contact one is in the claustrum). PT5 is a white matter contact of the electrode (posterior temporal) in the contralateral hemisphere (PT is a reference). Black arrows are signaling HFO overriding the spike and wave complex in the claustrum during the postictal period.

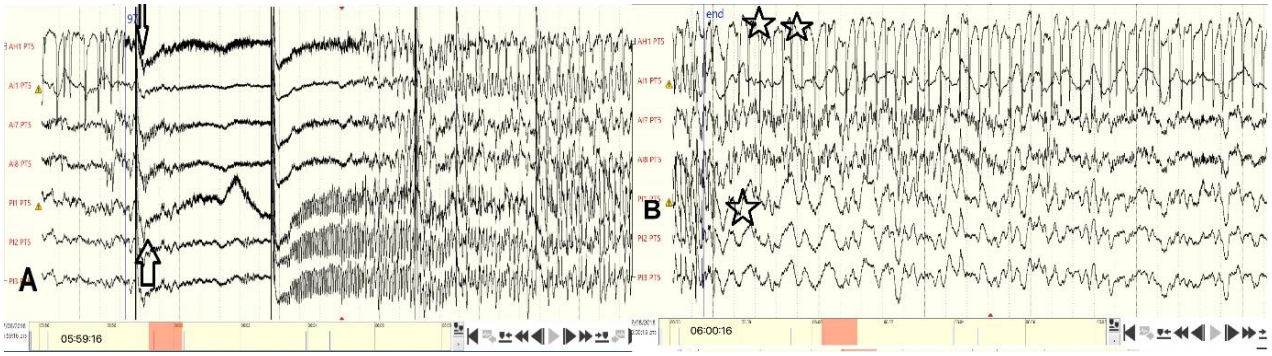


Figure 3 F: Early termination of claustrum ictal discharges seen in a patient with a cluster of seizures.
The patient is a 13-year-old with a focal seizure with impaired awareness. AH hippocampal head, AI anterior insular cortex, PI indicates the posterior insular cortex (contact one is in the claustrum). PT5 is a white matter contact of the electrode (posterior temporal) in the contralateral hemisphere (PT is a reference). The figure shows a focal seizure consisting of high amplitude 1-2 Hz periodic spike and wave in the hippocampus head followed by a sudden onset of diffuse low voltage fast activity. This pattern evolves into a higher amplitude 10-13 Hz rhythmic spikes that decrease in frequency progressively. Observe that the ictal onset occurs simultaneously in the hippocampal head, Claustrum (PI1), and AI 7-8 (located in the superior temporal gyrus). Figure F b shows that approximately at 06:00:16, there is some periodic epileptiform discharge in the claustrum. After three seconds, the claustrum spikes drop out, and a new seizure emerges in the hippocampus. Figures 3Fc and 3Fd show the same phenomenon and two other seizures occurring at 06:03:34 and 06:05:45. After four hours with subclinical recurrent seizures, periodic spikes with superimposed HFO are noted in the claustrum, and no other seizures were recorded (figure 3 F e and f).

If we can better clarify the role of the claustrum in the epileptogenic network this could have potential consequences for planning of resective surgery and future neuromodulatory targets. Based on the evidence generated in this study, we suggest that claustrum neuromodulation could possibly have an antiepileptic mechanism.

Limitations of this study include a retrospective nature with data limited to patients who had claustrum placement of SEEG electrodes based on the requirements of presurgical planning. It should be noted that in most patients with claustrum or insular electrode placement, this typically indicates the epilepsy team has suspicion for extra-temporal SOZ, which introduces selection bias. Another limitation of our study is that only one neurophysiology specialist carried out the ictal onset analysis. Another potential limitation is the surprising surgical results, with all

patients having poor seizure-free outcomes (Engel III or IV). This calls into question the quality of the patient selection for SEEG, the electrode implantation strategy, the conclusions drawn about the epileptogenic zone, the surgical strategy, or a combination of all of these. A study with good ictal onset zone localization and seizure-free outcomes would bring much more convincing data. However, all of these patients but one had temporal lobe epilepsy. We sampled the hippocampus, amygdala, entorhinal cortex, temporal pole superior, middle and inferior temporal gyrus with three electrodes in each gyrus, and the temporal plus zones including insular cortex, temporal occipital cortex, orbitofrontal cortex, and the operculum. Although there is no one standardized way to place these electrodes, they are strategically implanted based on patient ictal semiology, MRI and PET data, and ictal and interictal scalp EEG to reduce the possibility of sampling or analysis failure accounting for this postsurgical outcome. Another possibility is that the claustrum itself might play a role in this poor prognosis. Last, due to the sample bias inherent to SEEG electrode implantation, the possibility that seizures can originate close but not at the implantation site cannot be ruled out.

Conclusion

In conclusion, this study highlights the involvement of the claustrum in seizure propagation, offering new insights into epileptogenic networks. It remains to be determined whether the claustrum plays an excitatory or inhibitory role.

Acknowledgement

We confirm that we have read the Journal's position on issues involved in ethical publication and affirm that this report is consistent with those guidelines.The author responsible for the publication: Rene Andrade Machado M.D

AI Statement

During the preparation of this work, the author(s) do not use AI in order to write the manuscript.

Author Contributions

Rene Andrade Machado: Conceived the study design, , did the statistic analysis, reviews SEEG files, and MRI and drafted the manuscript and reviewed it critically for important intellectual content; and gave final approval of the version to be published

Jennifer Meylor, MD: Collected data discussed results, drafted the work and reviewed it critically for important intellectual content; and gave final approval of the version to be published

Conflict of interest

None of the authors has any conflict of interest to disclose

References

1. Wong AC, Ryan AF. Mechanisms of sensorineural cell damage, death and survival in the cochlea. Front. aging neurosci. 2015;7:58.
2. Le TN, Straatman LV, Lea J, Westerberg B. Current insights in noise-induced hearing loss: a literature review of the underlying mechanism, pathophysiology, asymmetry, and management options. J OTOLARYNGOL-HEAD N. 2017;46(1):1-15.
3. Oroei M, Ahadi M. Stem Cell Therapy in Children With Sensorineural Hearing Loss: A Narrative Review. J. Pediatr. Rev. 2021;9(3):219-28.
4. Mazaheryazdi M, Sharafi MA, Akbari M, Choobdar FA. Comparing Auditory Brain Stem Responses and Transient Otoacoustic Emissions in Premature Infants with Auditory Developmental Delay: Evidence of Temporary Auditory Neuropathy. Iran. J. Child Neurol. 2023;17(4):35.
5. Liaw YS, Augustine GJ. The claustrum and consciousness: An update. Int J Clin Health Psychol. 2023;23(4):100405.
6. Kurada L, Bayat A, Joshi S, Koubeissi MZ. The Claustrum in Relation to Seizures and Electrical Stimulation. Front Neuroanat. 2019;13:8.
7. Salerno MT, Cortimiglia R, Crescimanno G, Amato G, Infantellina F. Effects of claustrum stimulation on spontaneous bioelectrical activity of motor cortex neurons in the cat. Exp Neurol. 1984;86(2):227-39.
8. Witter MP, Room P, Groenewegen HJ, Lohman AH. Reciprocal connections of the insular and piriform claustrum with limbic cortex: an anatomical study in the cat. Neuroscience. 1988;24(2):519-39.
9. Smith JB, Alloway KD. Interhemispheric claustral circuits coordinate sensory and motor cortical areas that regulate exploratory behaviors. Front Syst Neurosci. 2014;8:93.
10. Majak K, Morys J. Endopiriform nucleus connectivities: the implications for epileptogenesis and epilepsy. Folia Morphol (Warsz). 2007;66(4):267-71.
11. Wada JA, Kudo T. Involvement of the claustrum in the convulsive evolution of temporal limbic seizure in feline amygdaloid kindling. Electroencephalogr Clin Neurophysiol. 1997;103(2):249-56.
12. Connell P, Bayat A, Joshi S, Koubeissi MZ. Acute and spontaneous seizure onset zones in the intraperitoneal kainic acid model. Epilepsy Behav. 2017;68:66-70.

13. Sheerin AH, Nylen K, Zhang X, Saucier DM, Corcoran ME. Further evidence for a role of the anterior claustrum in epileptogenesis. Neuroscience. 2004;125(1):57-62.

14. Watson GDR, Smith JB, Alloway KD. Interhemispheric connections between the infralimbic and entorhinal cortices: The endopiriform nucleus has limbic connections that parallel the sensory and motor connections of the claustrum. J Comp Neurol. 2017;525(6):1363-80.

15. Atilgan H, Doody M, Oliver DK, McGrath TM, Shelton AM, Echeverria-Altuna I, et al. Human lesions and animal studies link the claustrum to perception, salience, sleep and pain. Brain. 2022;145(5):1610-23.

16. Meletti S, Giovannini G, d'Orsi G, Toran L, Monti G, Guha R, et al. New-Onset Refractory Status Epilepticus with Claustrum Damage: Definition of the Clinical and Neuroimaging Features. Front Neurol. 2017;8:111.

17. Obara K, Wada C, Yoshioka T, Enomoto K, Yagishita S, Toyoshima I. Acute encephalopathy associated with ingestion of a mushroom, Pleurocybella porrigens (angel's wing), in a patient with chronic renal failure. Neuropathology. 2008;28(2):151-6.

18. Koubeissi MZ, Bartolomei F, Beltagy A, Picard F. Electrical stimulation of a small brain area reversibly disrupts consciousness. Epilepsy Behav. 2014;37:32-5.

19. Jayakar P, Gotman J, Harvey AS, Palmini A, Tassi L, Schomer D, et al. Diagnostic utility of invasive EEG for epilepsy surgery: Indications, modalities, and techniques. Epilepsia. 2016;57(11):1735-47.

20. Engel J, Jr. Classification of epileptic disorders. Epilepsia. 2001;42(3):316.

21. Hirsch LJ, Fong MWK, Leitinger M, LaRoche SM, Beniczky S, Abend NS, et al. American Clinical Neurophysiology Society's Standardized Critical Care EEG Terminology: 2021 Version. J Clin Neurophysiol. 2021;38(1):1-29.

22. Sperner J, Sander B, Lau S, Krude H, Scheffner D. Severe transitory encephalopathy with reversible lesions of the claustrum. Pediatr Radiol. 1996;26(11):769-71.

23. Meletti S, Slonkova J, Mareckova I, Monti G, Specchio N, Hon P, et al. Claustrum damage and refractory status epilepticus following febrile illness. Neurology. 2015;85(14):1224-32.

24. Nixon J, Bateman D, Moss T. An MRI and neuropathological study of a case of fatal status epilepticus. Seizure. 2001;10(8):588-91.

25. Zhang X, Hannesson DK, Saucier DM, Wallace AE, Howland J, Corcoran ME. Susceptibility to kindling and neuronal connections of the anterior claustrum. J Neurosci. 2001;21(10):3674-87.

26. Mohapel P, Zhang X, Gillespie GW, Chlan-Fourney J, Hannesson DK, Corley SM, et al. Kindling of claustrum and insular cortex: comparison to perirhinal cortex in the rat. Eur J Neurosci. 2001;13(8):1501-19.

27. Cortimiglia R, Crescimanno G, Salerno MT, Amato G. The role of the claustrum in the bilateral control of frontal oculomotor neurons in the cat. Exp Brain Res. 1991;84(3):471-7.

28. Bruno RM. Synchrony in sensation. Curr Opin Neurobiol. 2011;21(5):701-8.